Effect of Surfactant on FRET and Quenching in DNA Sequence Detection Using Conjugated Polymers

ARTICLE *in* ADVANCED FUNCTIONAL MATERIALS · SEPTEMBER 2008

Impact Factor: 11.81 · DOI: 10.1002/adfm.200700809

2 AUTHORS:

Hameed Al Attar
Durham University
17 PUBLICATIONS **324** CITATIONS
SEE PROFILE

Andy Monkman
Durham University
415 PUBLICATIONS **9,678** CITATIONS
SEE PROFILE

ADVANCED FUNCTIONAL MATERIALS

FULL PAPER

DOI: 10.1002/adfm.200700809

Effect of Surfactant on FRET and Quenching in DNA Sequence Detection Using Conjugated Polymers**

By *Hameed A. Al Attar** and *Andy P. Monkman*

The effect of a nonionic surfactant on various energy-transfer and quenching processes in deoxyribonucleic acid (DNA) sequence detection using the cationic conjugated polymer (CCP) poly{[9,9-bis(*N*,*N*,*N*-trimethylammonium)hexylfluorene]-*co*-1,4-phenylene diiodide} and peptide nucleic acid labeled with fluorescein (PNA-Flu*) has been investigated. Steady-state and time-resolved measurements reveal that nonionic surfactant enhances both sensitivity and selectivity in targeted DNA sequence detection. The enhancement of the sensitivity is ascribed to an increase in the CCP quantum yield due to the surfactant breaking up polymer aggregates, increasing the isolated polymer chain concentration, and reducing interchain quenching. This also increases the polymer surface-to-volume ratio. The sensitivity is also improved as the surfactant reduces CCP quenching by DNA and buffer solution through incorporation of the CCP in micelles, which reduces charge-transfer processes. Enhancement of the selectivity is achieved through the reduction of the hydrophobic interaction between the CCP and free PNA-Flu*. Time-resolved fluorescence lifetime analysis provides an effective way to differentiate these particular effects in the DNA-PNA-Flu assays. Comparing the decay profiles of the CCP, CCP/DNA, and CCP/complementary DNA:PNA-Flu*, it was found that both surfactant and DNA do not alter dramatically the isolated polymer chain lifetime (the first increases the concentration of the single chains by breaking up the polymer aggregation and the latter reduces the concentration of the isolated polymer chain by static quenching), therefore the change in the isolated polymer chain fluorescence lifetime can predominantly reflect the quenching of the donor by FRET to the PNA fluorescent label. Here, surfactant increases Förster radius by enhancing the polymer fluorescence quantum yield. Furthermore, surfactant also increases the difference in the donor lifetimes between the complementary and noncomplementary cases. This difference reflects the increase in the energy-transfer efficiency and hence higher selectivity. Fluorescein quenching is mediated by the CCP which causes Flu*-Flu* self-quenching via a PNA-CCP hydrophobic interaction. Optimization or minimization of various interactions to achieve the best DNA detection sensor is discussed.

1. Introduction

Detection of specific oligonucleotide sequences underpins new approaches in genetic medicine, medical diagnosis, and environmental monitoring.[1–3] A wide range of techniques for detecting nucleic acid sequences based on their hybridization to complementary probes have been proposed. Several methods have been reported recently in DNA hybridization assays. These include thermodynamic methods that depend on differences in the melting profile,[4] electrochemical methods based on redox-active nucleic acids,[5,6] electronic detection based on the change in the DNA intrinsic molecular charge,[7] and colorimetric detection based on the difference in electrostatic interactions of double- and single-stranded oligonucleotides with nanoparticles.[8,9]

Recently, three methods of DNA sequence detection using cationic conjugated polymers (CCPs) have been proposed.[10–12] These methods are very versatile and show great promise for simple, high-sensitivity, and fast DNA detection. CCPs are specially synthesized conjugated polymers that have a sufficient density of polar substituents to render them soluble in a polar medium, such as water and/or methanol. The first method is based on different electrostatic interactions and conformational structures between the CCP, poly(3-alkoxy-4-methylthiophene)s, and single-stranded DNA (ss-DNA) or hybridized double-stranded DNA (ds-DNA).[10] Using this method Leclerc and coworkers have been able to detect and distinguish a specific sequence of oligonucletides having a single mismatch and in very low concentration.[11,12] The second method of detection is based on the difference in superquenching of the CCP in complementary and noncomplementary systems.[13] The third method of detection is based on optical amplification of a probe signal by light harvesting from a water-soluble conjugated polymer such as poly (9,9-bis(6'-*N*,*N*,*N*-trimethylammonium)hexylfluorenephenylene)

[*] Dr. H. A. Al Attar, Prof. A. P. Monkman
Organic Electroactive Materials Research Group
Department of Physics, University of Durham
South Road, Durham DH1 3LE (UK)
E-mail: h.a.al.attar@durham.ac.uk

[**] The authors thank Professor Ulli Scherf for the kind gift of the cationic conjugated polymer. They acknowledge the Medical Research Council (MRC) and CENAMPS for funding via the Durham University Photonic Materials Institute.

ADVANCED FUNCTIONAL MATERIALS

containing iodide or bromide counteranions.[14] Here sensitivity and selectivity of detection arise from the use of labeled peptide nucleic acids (PNAs). PNAs are DNA analogs where the four nucleotides (A, T, G, and C), are attached to a *N*-(2-aminoethyl)glycine backbone instead of the negatively charged deoxyribose phosphate backbone in DNA.[15,16] PNA has a high affinity and specificity when hybridized to complementary DNA and RNA, essentially because it is uncharged and has a flexible polyamide backbone. The detection procedure in this method[14] involves a solution containing nucleotides (ssPNA or ssDNA) labeled with fluorescent chromophore C*, and complementary or noncomplementary target ssDNA. If the DNA and nucleotides are complementary and hybridized the negatively charged DNA/PNA-C* or DNA/DNA-C* complex is electrostatically attracted to the CCP and the close proximity of the CCP to the C* label enables a fluorescence resonant energy transfer (FRET) process, that is, Förster energy transfer, to take place between the excited CCP donor and the nonexcited C* acceptor. The hybridized complex is therefore detected by enhanced emission from the PNA- or DNA-label acceptor. The positively charged CCP may also form a complex with the negatively charged free DNA, in which the CCP excited states can be quenched by forming a nonradiative complex in the ground state or by a charge-transfer process in the excited state.[17,18] CCP–CCP quenching may also occur when more than one CCP is bound to a DNA or DNA/PNA duplex. Hydrophobic interactions between macromolecules such as conjugated polymers and DNA or PNA are also possible and will reduce the selectivity between the complementary and noncomplementary DNA detection.[17] Typically, it is also found that CCP fluorescence quantum yields in water are up to an order of magnitude lower than in organic solvents.[20,21] Thus, optimization of the detection in these CCP/DNA:PNA-based assays is critically important when exploring the lower concentration threshold, and selectivity is of great importance for sensing small quantities of target DNA with a single base mismatch.

Three parameters should be optimized in order to fulfill the above requirements. First, the fluorescence quantum yields of the CCP should be increased, while the fluorescent quenching by DNA and water should be minimized. Second, energy transfer should be maximized by ensuring that the CCP emission and the fluorescent dye absorption have good spectral overlap for efficient FRET and by increasing the surface-to-volume ratio of the CCP to increase the interaction cross section, which can be done by breaking up aggregated chains. Third, reduction of the hydrophobic interactions is necessary to improve the selectivity between complementary and noncomplementary DNA:PNA. The hydrophobic interaction becomes effective only at relatively high oligonucleotide concentrations, and therefore very dilute conditions ensure improved selectivity, albeit at the expense of sensitivity. One method to improve the selectivity has been suggested in which the complementary and noncomplementary DNA:PNA-C* assays emit at different wavelengths.[22,23] Liu and Bazan[24] have studied the optimization of DNA detection by matching donor and acceptor orbital energy levels. This study gives a preliminary basis for understanding the competition between FRET and photoinduced charge transfer (PCT). Other methods to improve selectivity were proposed by Xu et al.,[19] by mixing a fraction of organic solvent, such as *N*-methylpyrrolidone (NMP) with the water. The energy-transfer efficiency for the noncomplementary DNA/PNA-Flu duplex was found to be greatly reduced, but unfortunately, the energy transfer (FRET) between the CCP and PNA-C* also become very inefficient. The interaction of surfactant with conjugated polyelectrolytes is known to enhance the polymer quantum yields in aqueous solution,[25,26] which has been explained as surfactant-induced breakup of polymer aggregates, reducing nonemissive interchain excitations that compete with emissive intrachain exciton formation and enhancing the PL quantum yield.[27] The surfactant may also reduce fluorescence quenching by water, by preventing nonradiative processes through incorporation of the polymer chains into micelles.[28]

In this paper, we discuss a method by which we have enhanced the detection of a targeted DNA sequence based on optical amplification of the probe signal by light harvesting from a water-soluble conjugated polymer using a nonionic surfactant. The mechanisms of energy transfer and quenching in the presence of surfactant are investigated. Steady-state and time-resolved fluorescence measurements were carried out and FRET parameters are calculated. A comparison of the sensitivity and selectivity of detection of complementary and noncomplementary ssDNA using labeled PNA is presented.

2. Results and Discussion

2.1. Material Photophysics and Detection System

The normalized absorption and emission spectra of the various materials used are shown in Figure 1. The emission of **1** (Scheme 1) possesses a tail that extends beyond 550 nm and overlaps with the fluorescein absorption band, fulfilling the FRET process requirement. Upon addition of the surfactant **2** (3.4×10^{-4} M) to **1** (1×10^{-5} M), the fluorescence emission of the CCP increases by a factor of 10. In addition, there is a ca. 10 nm blue shift of the emission maxima (Fig. 1, inset). We have shown[17] that nonionic surfactant enhances the photoluminescence (PL) quantum yield of the CCP **1** in water from $\Phi_f = 0.03$ to 0.23. In DNA sequence detection based on optical amplification of the probe signal by light harvesting from a water-soluble conjugated polymer, the FRET process is directly proportional to the hybridization state. The hybridization process is the key parameter for any efficient DNA sequence detection. Incomplete hybridization reduces the number of available FRET acceptors and increases the free DNA and PNA-Flu in the assay, which reduces both the sensitivity and the selectivity. In an assay of polyelectrolyte (CCP) containing complementary or noncomplementary

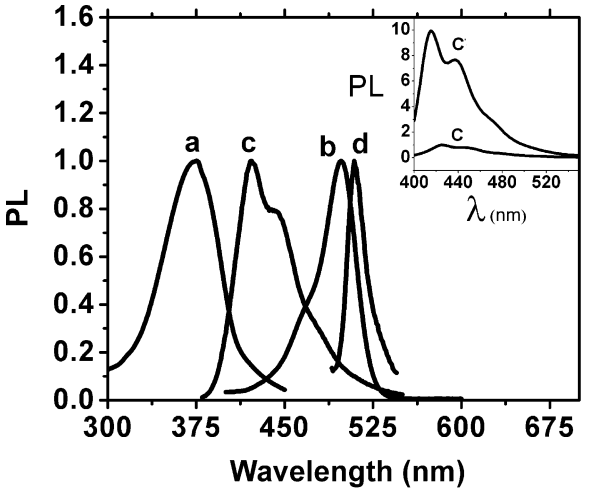

Figure 1. Steady-state normalized absorption and fluorescence spectra of polymer **1** (absorption, curve a; emission, curve c) and ssPNA-Flu probe **3** (absorption, curve b; emission, curve d). The PL emission spectra in the presence of surfactant (curve c′), normalized to that without surfactant (curve c), is shown in the inset. [CCP] = 1×10^{-5} M, [$C_{12}E_5$] = (3.4×10^{-4} M), λ_{exc} = 374 nm.

DNA:PNA-Flu, electrostatic and hydrophobic interactions generate various structures that influence the optical performance of the system. Some of the important structures are shown in Scheme 2A. The CCP (blue) can be in multiple phases, namely, isolated polymer chains, partially dissolved polymer (clusters), and aggregated polymer.[17] The latter two may be considered as interchain species. Also depicted is free DNA (red) and PNA-Flu* (black, 2). The gray lines in the second row represent surfactant. The blue and green flashes represent the fluorescence emission of the donor CCP and the acceptor fluorescein. Electrostatic interactions between CCPs and the negative phosphate groups in hybridized and non-hybridized DNA/PNA-Flu may form structures such as CCP/DNA (3) and CCP/DNA:PNA-Flu (5). Aggregated CCP at a DNA nucleation site (4) or aggregated DNA/PNA-Flu* at a CCP site (6) is also possible. Structure 5 (Scheme 2) provides the close proximity that is required for an efficient FRET process. In structure 3 the donor fluorescence is strongly quenched by charge transfer to the DNA. Self-quenching of the donor polymer (CCP...CCP) and acceptor labels (C*...C*),

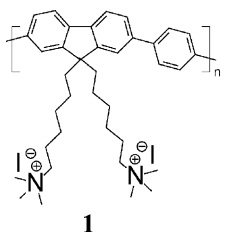

1

$H\text{-}(OCH_2CH_2)_5OCH_2(CH_2)_{10}CH_3$ **2**
$C_{12}E_5$

Flu-OO-AGT-AAC-TCA-AGT-3` **3**
DNA1, 5`-ACT TGA GTT ACT-3` **4**
DNA2, 5`-CTC CAA CGT CTA-3` **5**

Scheme 1. Chemical structures of the water-soluble polyfluorene poly{9,9-bis[*N*,*N*-trimethylammonium)hexyl]fluorene-*co*-1,4-phenylene diiodide} (CCP) **1**, the nonionic surfactant *n*-dodecylpentaoxyethylene glycol ether ($C_{12}E_5$) **2**, PNA-Flu* **3**, and the complementary and noncomplementary DNAs **4** and **5**.

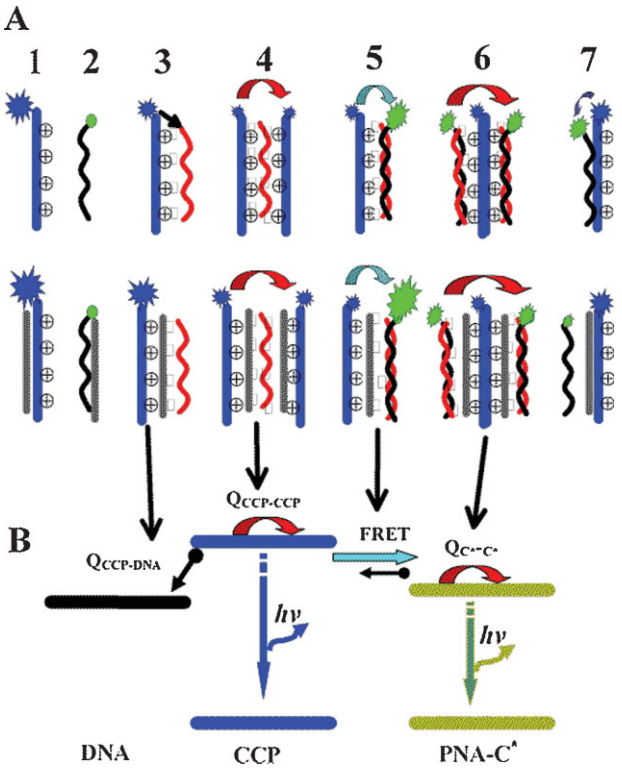

Scheme 2. A) The expected constituents and the possible interactions between CCP/DNA:PNA-Flu* in an assay without surfactant (first row) and with surfactant (second row). The symbols are explained in the text. B) Hypothetical schematic energy diagram showing energy- and charge-transfer processes and quenching mechanisms.

which leads to a decrease in the FRET signal, is depicted in structures 4 and 6, respectively. Finally, hydrophobic interactions may lead to the formation of structure 7, which reduces the selectivity of the detection between the complementary and noncomplementary systems. The CCP is a hydrophobically modified polymer, which by itself has interesting aggregation behavior that leads to interchain interaction and reduces CCP quantum yield.[17] The CCP may interact with various constituents, depending on size, shape, and charge. The estimated CCP **1** diameter (chain length) using small-angle neutron scattering[29] is about 3 nm. The size of 12-base DNA or PNA, based on the average size of a single base being 3 Å, is about the size of one pitch, 3.6 nm.[30] These comparable sizes of the CCP and DNA or PNA reduce the possibility of forming various sizes of CCP/DNA or CCP/PNA complexes. However, due to aggregation of CCP–CCP and DNA–DNA by hydrophobic interactions in water, complexes containing multiple CCP chains with one DNA or multiple DNA or DNA:PNA-Flu* around a single CCP are possible structures. Self-quenching of aggregated CCP and aggregated DNA:PNA-Flu* may occur, which also has a strong effect on the detection process. The dominant interaction will be energy transfer from CCP to Flu by efficient FRET when the CCP and PNA-Flu are within the Förster radius. Static quenching and charge transfer due to complex formation also play a strong role in the CCP quenching by DNA or DNA:PNA-Flu* but occurs over a much shorter range.

ADVANCED FUNCTIONAL MATERIALS

2.2. Effect of Surfactant on the Sensitivity and Selectivity of the Detection

At very low CCP concentration, the FRET process is suppressed due to a strong static quenching of the CCP by the free DNA. At a specific CCP concentration, depending on the hybridization level, an abrupt increase in the FRET occurs and strong amplification of the fluorescein emission can be obtained. This implies that, in an incompletely hybridized assay, quenching by the free DNA is the dominant process, which reduces the energy transferred to the acceptor. The organic core of the conjugated polymer is only partially shielded by the hydrophilic side groups. Therefore, the CCP may display hydrophobic interactions, leading to the formation of weakly aggregated polymer chains. We have shown[17] that nonionic surfactants such as $C_{12}E_5$ rapidly break up these aggregates, indicating that the forces holding CCP in an aggregate form are weak. In the work presented here we investigated how small-molecule nonionic surfactant can improve the sensitivity and selectivity of the detection of a specific DNA sequence.

Figure 2 shows the complementary and noncomplementary assays in the absence of surfactant (a) and in the presence of surfactant (b). The results indicate that the most efficient FRET process occurs for the complementary assays with surfactant (Fig. 2b, curve 2). Importantly, the acceptor emission for the noncomplementary assay (Fig. 2b, curve 1) is greatly reduced in the presence of surfactant, compared with that in the absence of surfactant (Fig. 2a, curve 1). These results indicate that increased sensitivity and selectivity are achieved by the introduction of surfactant. Increasing the concentration of CCP may enhance the sensitivity but reduces the selectivity due to the CCP–PNA-Flu* proximity caused by high concentration. Therefore, addition of surfactant is the best way to keep good selectivity *and* sensitivity. Due to the strong FRET in the present of surfactant, complementary DNA can be detected visually as a green-light-emitting solution — as opposed to a blue-light-emitting solution for the noncomplementary DNA — in the assay when excited by light at 370 nm. A FRET ratio, defined as the ratio of PL emission at 526 nm to that at 420 nm, for complementary DNA:PNA-Flu* assays ($[1 \times 10^{-7}$ M]) as a function of a donor CCP concentration is shown in Figure 3. The FRET ratio first increases then drops as the donor concentration far exceeds that of the acceptor. The FRET ratio for the complementary assay in the presence of surfactant is three times that without surfactant, which reflects the enhancement in the FRET process. In the presence of surfactant, the maximum FRET ratio occurs at a CCP concentration a factor of 3–4 lower than that seen in the absence of the surfactant. This indicates that CCP aggregation acts to lower the effective concentration. Furthermore, the dependence is much less pronounced in the case of pure CCP, owing to the wide distribution of the sizes of the aggregated chains compared with the narrow distribution in the presence of surfactant, where isolated polymer chains are dominant in the interaction with DNA:PNA-Flu*.

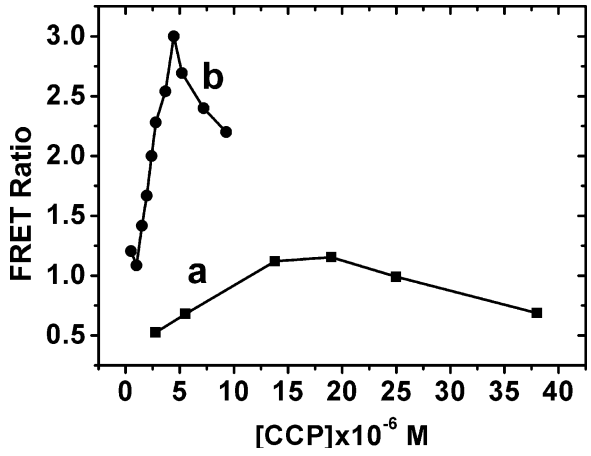

Figure 3. FRET ratio measured as a function of [CCP]; the concentration of complementary DNA:PNA-Flu* was kept constant at 1×10^{-7} M. Fluorescence was measured by excitation at 374 nm. Measurements were performed in 10 mM phosphate buffer in the absence (curve a) and presence (curve b) of surfactant ($[C_{12}E_5] = 1 \times 10^{-4}$ M).

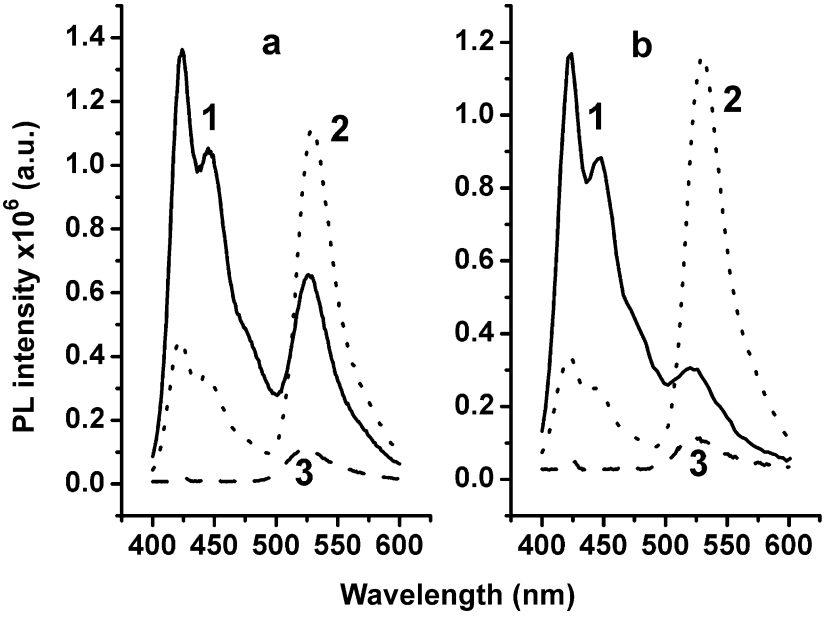

Figure 2. The noncomplementary (curve 1) and complementary (curve 2) assays, in the absence (a) and presence (b) of surfactant ($[C_{12}E_5] = 1 \times 10^{-4}$ M). Curve 3 is the assay before the CCP was added. Excitation wavelength $\lambda_{exc} = 374$ nm.

The influence of the surfactant on the sensitivity and the selectivity of detecting specific DNA sequences is shown in Figure 4. The result is normalized with respect to the CCP peak emission. An enhancement in sensitivity *and* selectivity is clearly shown between the complementary and noncomplementary assays when surfactant is used. An enhancement in selectivity with surfactant was also observed in DNA with a single base mismatch.[31] Other nonionic surfac-

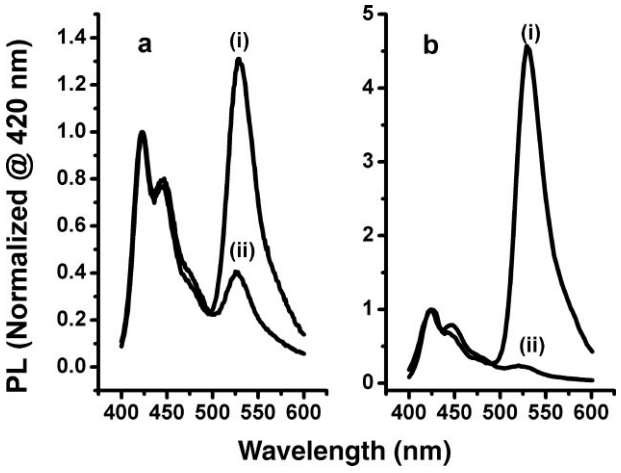

Figure 4. Emission spectra of the CCP/DNA:PNA-Flu* assay in the absence (a) and presence (b) of surfactant ($[C_{12}E_5] = 1 \times 10^{-4}$ M) for complementary (curves i) and noncomplementary (curves ii) DNA. $\lambda_{exc} = 374$ nm. The spectra are normalized with respect to the CCP emission.

tants such as Brij 35 and Triton-X have similar effects on CCP quantum yield and improve DNA detection. However, comparison between $C_{12}E_5$ and Brij 35 ($C_{12}E_{23}$) shows that larger surfactant molecules are less effective and the enhanced quantum yield decreases over time. The reason is not well understood but it is probably due to the formation of large micelles that grow with time and tend to precipitate the CCP polymer chains, or large micelles that may quench the CCP. This property does not affect the detection sensitivity but does affect the long-term stability of the CCP/surfactant mixture.

2.3. Effect of Surfactant on Energy- and Charge-Transfer Processes in DNA Sequence Detection

In order to determine the processes responsible for maximizing or minimizing the sensitivity and selectivity of the DNA sequence detection, various energy-transfer and quenching mechanisms were evaluated in the presence of surfactant. The hypothetical schematic energy diagram in Scheme 2B shows various possible interactions, including energy- and charge-transfer and quenching mechanisms between the most likely constituents in the assay. The second row of Scheme 2A shows the predicted structures in the presence of surfactant. The strong energy transfer process (FRET, 5), occurring from CCP to the fluorescein label is enhanced by surfactant, due in part to the enhancement in CCP quantum yield and the increase of surface-to-volume ratio (increase of isolated polymer chains). This process was confirmed by measuring the fluorescence decay profile of the CCP emission in the presence and absence of surfactant. Figure 5 shows the decay profile of the CCP in water for the complementary (curve iii) and noncomplementary (curve ii) DNA assays without (a) and with (b) surfactant. The results show clearly the difference in the decay profile in the two assays. As CCP quenching is not wholly due to the energy transfer by FRET, we should evaluate other possible processes that induce quenching in the CCP and discuss the effect of surfactant on these processes. The large difference in the decay profiles of the noncomplementary DNA assay (Fig. 5, curve ii) in (a) and (b) clearly indicates that surfactant eliminates strong quenching components to the CCP. Comparison with the steady-state PL of Figures 2 and 4 suggests that this component is partly due to a hydrophobic interaction between free PNA-Flu* and CCP. Time-resolved analysis can be used to demonstrate the effect of surfactant on DNA sequence detection quantitatively. In order to differentiate the particular effects on the DNA-PNA-Flu assays, a time-resolved analysis was employed to study first the effect of surfactant and ssDNA on the donor (CCP) fluorescence. Time-resolved fluorescence decay measurements at 420 nm for the CCP and CCP/DNA system were performed and the data were fitted with three discrete exponential terms, $j = 3$, using global analysis:

$$I(t) = \sum_{i=1}^{j} a_i \exp(-t/\tau_i) \quad (1)$$

where $I(t)$ is the intensity at time t, the a_i represent the amplitudes of the components i at $t = 0$, and τ_i is the decay time of the component i. In our detailed analysis of the effect of nonionic surfactant on the conjugated polymer, we have shown that CCP exists in water in at least three phases: isolated polymer chains, an aggregated form (solid state), and variable-size clusters. The enhancement of the PL quantum yield of the CCP in water is due to breakup of polymer aggregates, which increases the concentration of the long-lived isolated polymer chains.[17] The three CCP phases have three time constants, which are around 600, 200, and 15 ps. The shortest time constant is for the CCP emission at 420 nm quenched by interchain interaction in the polymer aggregates. Surfactant reduces the contribution of this component by breaking up the polymer aggregation, as shown in the initial fast-decay region in Figure 6. Examples

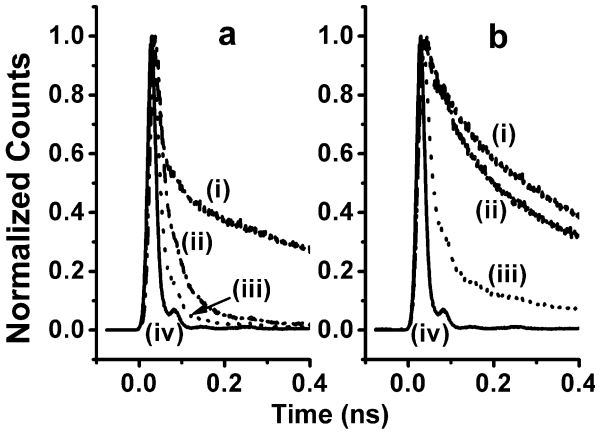

Figure 5. Decay profiles of pure CCP (i), CCP in noncomplementary assay (ii), and complementary assay (iii), in the absence (a) and presence (b) of surfactant ($[C_{12}E_5] = 1 \times 10^{-4}$ M). Curve iv is the excitation pulse at $\lambda_{exc} = 390$ nm.

ADVANCED FUNCTIONAL MATERIALS

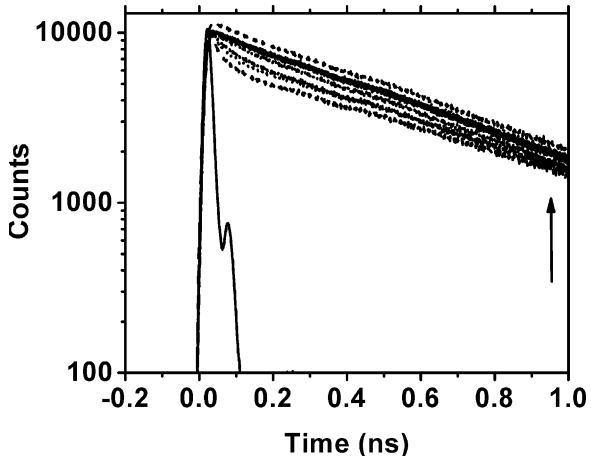

Figure 6. Decay time profile of the CCP **1** (5.5×10^{-5} M) in water at different surfactant concentrations (0 to 9×10^{-4} M). The arrow indicates increase in surfactant concentration. $\lambda_{exc} = 390$ nm.

of fitting results using global analysis for the data of Figure 6 are given in Table 1. Upon addition of DNA, the contribution of this component increases again, owing to polymer aggregation at the negatively charged DNA, leading to possible CCP–CCP quenching, as shown in the initial region of Figure 7. Examples of fitting results using global analysis for the data of Figure 7 are given in Table 2. This component reduces energy transfer as the quenching competes with

Table 1. Examples of fitting results using global analysis for the data of Figure 6.

$[C_{12}E_5]$ [M]	a_1	τ_1 [ps]	a_2	τ_2 [ps]	a_3	τ_3 [ps]	χ^2	$\langle\tau\rangle$ [ps]
0	50	644	109	18	9	203	1.1	620
9.6×10^{-4}	43	593	26	26	23	388	1.1	540
2×10^{-3}	39	595	25	29	28	405	1.07	532

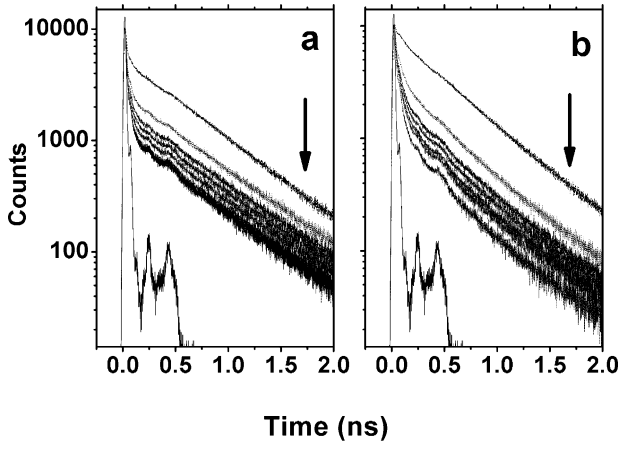

Figure 7. Decay-time profile of the CCP **1** (5.5×10^{-5} M) in water at different ssDNA concentrations (0 to 7.4×10^{-8} M) in the absence (a) and presence (b) of surfactant. The arrow indicates increase in ssDNA concentration. $\lambda_{exc} = 390$ nm.

Table 2. Examples of fitting results using global analysis for the data of Figure 7.

	[DNA] [M]	a_1	τ_1 [ps]	a_2	τ_2 [ps]	a_3	τ_3 [ps]	χ^2	$\langle\tau\rangle$ [ps]
(a)	0	54	590	17	73	317	7	1.1	534
	1.25×10^{-8}	44	640	24	90	580	9.3	1.1	511
	5.5×10^{-8}	32	634	32	90	1247	8.3	1.09	407
(b)	0	56	548	26	152	116	8	1.19	490
	1.25×10^{-8}	44	542	66	108	357	12	1.16	390
	5.5×10^{-8}	35	454	109	70	736	10	1.11	254

FRET. The intermediate time constant of ca. 200 ps is related to the polymer in cluster form, which is partially dissolved polymer. Surfactant increases the contribution and lifetime (200 to 400 ps) of this component by reducing the average size of the clusters, making them closer to the isolated polymer chains. Upon addition of DNA the lifetime is again reduced by cluster aggregation around DNA. We also believe some charge transfer may enhance the quenching of this component as a result of the imperfect complex formation between the DNA and cluster CCP (the DNA is not fully accessible to all CCP chains in the cluster to form a ground-state complex). The final decay component (600 ps), which represents the isolated polymer chain lifetime, is the most effective component in the energy-transfer process due to its intrinsically long lifetime and hence high fluorescence quantum yield. In the presence of DNA the lifetime of this component does not change very much (see the long tail decay and also confirmed by the fitting analysis, Fig. 7a), and only the amplitude is reduced, which indicates that static quenching occurs by complex formation in the ground state between the isolated polymer chain CCP and DNA. For CCP with surfactant, the presence of DNA induces a limited lifetime shortening, which is ascribed to CCP–CCP quenching and/or a dynamic quenching of the high isolated polymer chain population generated by the surfactant effect. This suggests using a lower concentration of the CCP when using surfactant to avoid CCP aggregation around the DNA, which leads to strong CCP–CCP quenching.

The average fluorescence lifetime can be estimated using

$$\langle\tau\rangle = \frac{\sum a_i \tau_i^2}{\sum a_i \tau_i} \tag{2}$$

The fitting results using global analysis[32] for a selected pure CCP and ssDNA/CCP in water in the presence and absence of surfactant are shown in Figures 6 and 7, respectively.

Time-resolved fluorescence decay measurements at 420 nm for the CCP "donor" emission and 520 nm for fluorescein "acceptor" emission were performed at room temperature, with excitation at 390 nm for the CCP in the presence of the complementary and noncomplementary DNA:PNA-Flu systems. A global analysis of the fluorescence decay of the two data sets is fitted simultaneously with four discrete lifetimes

using Equation 1, and the four lifetimes are "linked" across the data sets. In this analysis the lifetimes of the two sets stay the same and only their fractional contributions change in the donor and acceptor emission spectra. An example of a donor and acceptor emission decay together with the fitting results is shown in Figure 8. The fluorescence resonance energy transfer (FRET) rate (K_{FRET}) from a donor to an acceptor positioned at a distance r_{DA} is described by the long-range excitation energy transfer from the donor to acceptor via the dipole–dipole interaction, which is described by the Förster formula:[33]

$$K_{FRET} = \frac{1}{\tau}\left(\frac{R_0}{r_{DA}}\right)^6 \quad (3)$$

$$R_0 = \left[\frac{9000(\ln 10)Q_D\kappa^2 J(\lambda)}{128\pi^5 N n^4}\right]^{1/6} \quad (4)$$

$$J(\lambda) = \frac{\int_0^\infty F_D(\lambda)\varepsilon_A(\lambda)\lambda^4 d\lambda}{\int_0^\infty F_D(\lambda)d\lambda} \quad (5)$$

where τ_D is the lifetime of the donor in the absence of the acceptor, Q_D is the quantum yield of the donor in the absence of the acceptor, N is Avogadro's number, n is the refractive index of the medium, and κ^2 is a factor describing the relative orientation of the transition dipoles of the donors and acceptor. The integral $J(\lambda)$ expresses the degree of spectral overlap between the emission of the donor $F_D(\lambda)$ and the absorption of the acceptor $\varepsilon_A(\lambda)$. R_0 is referred to as the Förster distance. The Förster formula indicates that, for better energy transfer, the donor–acceptor distance r_{DA} should be very small, 10–100 Å, the donor lifetime should be short, and R_0 should be large (i.e., high donor fluorescence quantum yield and maximum spectral overlap). However, there is an optimum r_{DA} below which nonradiative contact quenching occurs by energy or electron transfer between the donor and acceptor, which reduces the FRET efficiency.[34] Therefore one expects that introducing a very thin layer between the donor and acceptor should suppress contact quenching and provide optimum FRET efficiency. However, to understand how surfactant enhances the rate of FRET we need to understand the quenching mechanism of CCP by DNA and by the hybridization buffer (phosphate buffer in our case), as well as to discuss the effect of surfactant on each parameter in Equations 1–3 separately.

If the surfactant encapsulates the CCP in a micelle this will increase the distance between the donor and the acceptor and hence reduce the rate of FRET. Therefore the enhancement of FRET in the presence of surfactant should come from the other factors. It is known that the effect of nonionic surfactant on the water-soluble conjugated polymers increases the fluorescence quantum yield and so increases the average lifetime.[33] However, the increase in fluorescence quantum yield with increasing surfactant concentration is valid for concentrations below 2 cmc (critical micelle concentration); above this value no further fluorescence enhancement was observed. Therefore there is an optimum surfactant concentration beyond which FRET will decrease. The energy transfer efficiency can be calculated using the relationship(6)

$$E_{DA} = 1 - \frac{\tau_D}{\tau_{DA}}$$

where τ_D and τ_{DA} are the measured decay lifetime of the donor in the absence and presence of the acceptor, respectively. The energy transfer efficiency can also be expressed in terms of energy transfer rate:

$$E_{DA} = \frac{k_T}{\tau_D^{-1} + k_T} \quad (7)$$

Using Equations 3–7, the distance between the donor and acceptor can be calculated from

$$r_{DA} = \frac{R_0}{(k_T - \tau_D)^{1/6}} \quad (8)$$

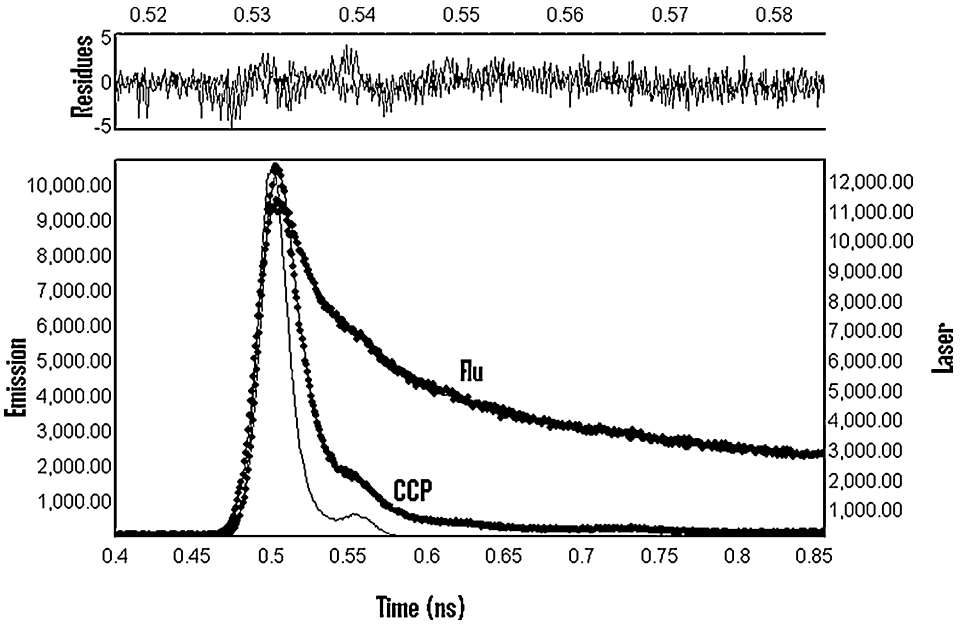

Figure 8. Example of the donor (CCP) "red" and the acceptor (fluorescein) emission "blue" decay, together with the fitted and residual curves. $\lambda_{exc} = 390$ nm.

ADVANCED FUNCTIONAL MATERIALS

In order to calculate the energy transfer efficiency between the donor and acceptor E_{DA} and hence the FRET rate coefficient k_T and the distance r_{DA} we need to define the decay lifetime of the donor in the presence of the acceptor. This system is, however, different from conventional two-point chromophores (dipoles) separated by a specific distance. The quenching of the donor is not totally due to energy transfer (FRET) to the acceptor. Other routes, such as complex formation and charge transfer to negatively charged DNA and phosphate ions, quench a large quantity of donor fluorescence. The steady-state measurement of the fluorescence decay of the donor emission at 420 nm as a function of ssDNA concentration indicates a strong quenching by ssDNA due to electrostatic complex formation. Further evidence for the contribution of electrostatic complex formation is provided by the observation that increases in ionic strength significantly reduce quenching efficiency due to ionic screening.[17] The calculated association constant K_S for this process, assuming the Stern–Volmer relation, $PL_0/PL = 1 + K_s[\mathrm{DNA}]$, was found to be $K_S = 5 \times 10^7\,\mathrm{M}^{-1}$, where PL_0 refers to overall integrated emission in the absence of DNA and PL corresponds to the intensity in the presence of the DNA. As the DNA concentration increases above 1×10^{-8} M, K_S decreases to a lower value: $2 \times 10^7\,\mathrm{M}^{-1}$. For the CCP with surfactant, the DNA quenching occurs at a lower rate: $1.1 \times 10^7\,\mathrm{M}^{-1}$. To clarify further the quenching mechanism, the τ_0/τ ratio obtained from the time-resolved quenching data, where τ_0 and τ are the CCP decay times in the absence and presence of the DNA respectively, is also plotted as a function of DNA concentration in Figure 9b obtained from the time-resolved quenching data shown in Figure 7 is plotted as a function of DNA concentration in Figure 9b. The time-resolved data show that the CCP with surfactant is quenched at a higher rate than that without surfactant, which contradicts the steady-state results. This indicates that steady-state analysis gives misleading results owing to the fact that surfactant increases the effective donor concentration, which reduces the influence of the static quenching on the DNA sequence detection. However, we believe that the high quenching rate of the CCP fluorescence in the presence of DNA is due to complex formation in the ground state and photoinduced charge transfer to the guanine residue,[17,35] as well as CCP–CCP aggregation quenching.[24,36] These processes need more experiment and analysis to differentiate the various quenching mechanisms, which we will not explore fully in this work. Quenching by charge transfer that occurs because of lack of accessibility between the DNA and CCP is a short-range process; we estimated it to be effective for a mean distance of less than 10 Å, similar to that found for an anionic sulfonated poly(*p*-phenylene vinylene), MPS-PPV, quenched by the cationic molecule methylviologen (MV^{2+}).[36] CCP–CCP quenching would arise if CCP aggregates were formed by nucleation on the DNA. Thus the correct balance between CCP and DNA: PNA-Flu concentrations to achieve the correct 1:1 stoichiometric system will prevent CCP from forming aggregates.

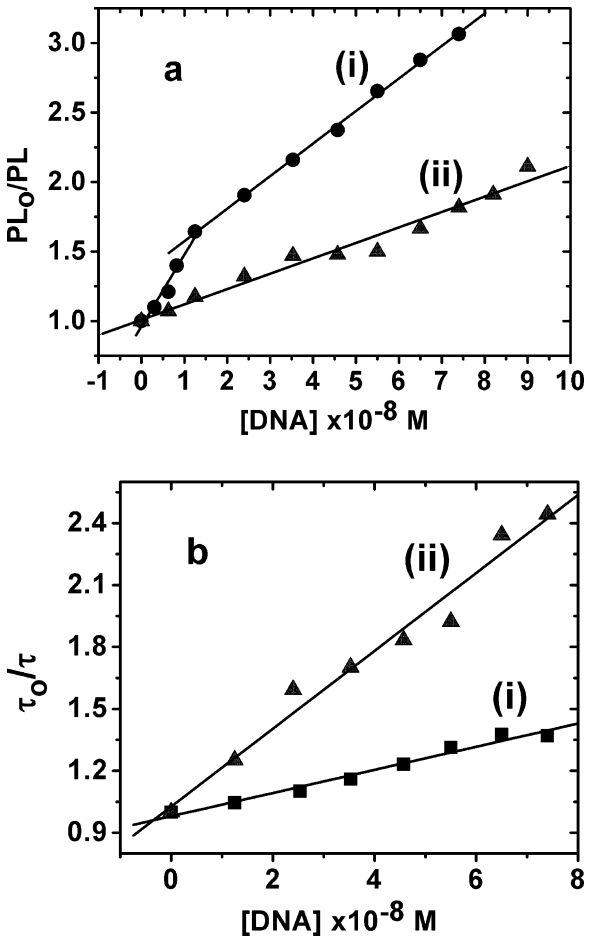

Figure 9. Stern–Volmer plots for a) steady-state PL and b) lifetime, showing the difference caused by the surfactant due to the changes of donor (isolated polymer chain) concentration. Curve i: without surfactant. Curve ii: with surfactant ($[C_{12}E_5] = 1 \times 10^{-4}$ M). $\lambda_{exc} = 374$ nm.

Quenching by mechanisms other than the static effect predominantly appears as an increase in the initial slope of the donor fluorescence decay (affecting the fast decay components) (Fig. 7). Surfactant reduces the strength of this quenching (see the value of a_3 in the associated result in Fig. 7) by incorporating the CCP into surfactant micelles, which increases the distance between the CCP and the DNA and prevents quenching by a photoinduced charge-transfer process. Fortunately, as both surfactant and DNA do not alter dramatically the isolated polymer chain lifetime (they simply reduce the isolated polymer chain concentration), the change in the long-lifetime component (600 ps) can predominantly reflect the quenching of the donor by FRET to the complementary and noncomplementary DNA:PNA-Flu* in the presence and absence of the surfactant. Considering only the isolated polymer chain CCP lifetime in the calculation of the rate of energy transfer and donor–acceptor distance, rather than the average lifetime, provides a more accurate estimate of the energy transfer efficiency by reducing the effect of CCP quenching by routes other than FRET. It should be noted that the isolated

polymer chain lifetime is slightly reduced by surfactant due to partial screening of the solvent polarity.[17] The calculated results for all cases are shown in Table 3, where the donor lifetime without the acceptor is considered to be 600 ps without surfactant and 580 ps with surfactant in order to account for the lifetime shortening due to water polarity reduction.

The quantum yield in the presence of surfactant was 10 times that without surfactant mainly due to break-up of the polymer aggregation and has been taken from our previous measurements.[17] The small difference between the overlap function $J(\lambda)$ is due to the fact that surfactant induces a 10 nm blue shift in the CCP fluorescence spectra emission, which reduces the normalized overlaps between the donor emission and acceptor absorption. Considering the average lifetime rather than the isolated polymer chain lifetime component that is responsible for FRET leads to an underestimate of the donor–acceptor distance r_{DA}. Table 3 demonstrates the effect of surfactant on the donor–acceptor distance and other Förster parameters. The largest difference between the isolated lifetime and the average lifetime (τ_{DA} and $\langle\tau_{DA}\rangle$) occurs for the complementary assay without surfactant (211 and 108 ps). This is due to a strong non-FRET quenching, that is, charge transfer and CCP–CCP quenching. This difference between τ_{DA} and $\langle\tau_{DA}\rangle$ is reduced (378 and 311 ps) by using surfactant because the non-FRET quenching is reduced. In the noncomplementary case the donor decay lifetime is longer, which demonstrates that very little FRET quenching takes place. Furthermore, the difference between τ_{DA} and $\langle\tau_{DA}\rangle$ is smaller since the quenching is predominantly charge transfer and CCP–CCP. Surfactant enhances the donor decay lifetime difference between the complementary and noncomplementary assays. Table 3 also shows that the difference for the efficiency of energy transfer E_{DA} between the complementary and noncomplementary assays is bigger for the assay with surfactant. This result demonstrates the enhancement in detection upon using surfactant. Taking the approximation that both surfactant and DNA do not alter the isolated polymer chain fluorescence lifetime too much, the effect of quenching by charge transfer and CCP–CCP can be seen to be reduced or eliminated by using surfactant. This effect can only be demonstrated by time-resolved analysis; the steady-state fluorescence measurement cannot resolve various sources of quenching.

The final question remaining is why the isolated polymer chain lifetime in the noncomplementary assay is quenched (288 ps). We ascribed this to the FRET from CCP bound to PNA-Flu by a hydrophobic attraction. This quenching mechanism can be dramatically reduced by surfactant (470 ps), which inhibits the CCP/PNA interaction, giving better selectivity of the detection. Therefore the presence of surfactant enhances both sensitivity and selectivity of detection, as we show in Figures 2, 3, and 5. Using the isolated polymer chain lifetime rather than the average lifetime reduces but does not completely eliminate the non-FRET quenching, especially in the presence of the surfactant, owing to a probable dynamic quenching, which may play some role as the concentration of the isolated single chain polymer increases with addition of surfactant. This is seen as a reduction in the lifetime with increasing surfactant concentration (Fig. 9b). However, increasing the surfactant beyond a specific value (which depends on the CCP molecular weight and concentration) reduces the sensitivity, owing to an increase in the donor–acceptor separation. This implies that the amount of surfactant required for optimum FRET ratio needs to be carefully adjusted.

The above analysis is only to demonstrate the effect of surfactant on the sensitivity and the selectivity of DNA sequence detection. Still higher quantitative accuracy requires the elimination of various non-FRET quenching processes from the total quenching. There may also be some small error due to other factors such as quenching of CCP by ssDNA, which is not the same as that by the complementary DNA:PNA owing to the difference in the DNA conformation (random or helical).

Returning to Figure 5b, we ascribe the small change in the decay profile (ii) for the noncomplementary DNA in the presence of surfactant to the surfactant eliminating the hydrophobic interaction that is responsible for energy transfer from the CCP to the PNA-Flu*. Just as DNA or DNA:PNA-Flu may attract more than one CCP, thus causing CCP–CCP quenching, single CCP may also attract more than one complementary DNA/PNA-Flu*, which may cause Flu*–Flu* self-quenching (Scheme 2, structure 6) and CCP-Flu dynamic quenching. To evaluate this quenching process we compared the fluorescein emission at two different excitation wavelengths, 374 nm (Fig. 10a) and 482 nm (direct excitation of fluorescein, Fig. 10b). The result shows that the excitation of the donor (CCP) at 374 nm induces efficient FRET to the acceptor (fluorescein) in the complementary DNA:PNA-Flu* system as expected (Fig. 10a), whereas the direct excitation of the acceptor (PNA-Flu*) at 482 nm shows strong fluorescein emission quenching upon successive addition of the CCP.

Although FRET is the dominant process, fluorescein quenching is very efficient, as shown in Figure 10b, which

Table 3. Förster parameters and the measured donor lifetimes in the presence (W/S) and absence (W) of surfactant. The energy transfer efficiency and the donor–acceptor distance for the complementary and noncomplementary assays were calculated using the isolated polymer chain fluorescence lifetime τ_{DA} and the average lifetime $\langle\tau_{DA}\rangle$ for comparison.

Assay	CCP Solvent	τ_{DA} ps	$\langle\tau_{DA}\rangle$ ps	$\Phi_{PL(D)}$	$J(\lambda)$	E_{DA}	$\langle E_{DA}\rangle$	R_o Å	r_{DA} Å	$\langle r_{DA}\rangle$ Å
Compl.	W	211	108	0.023	5.9×10^{14}	0.65	0.82	25	22.8	19.5
	W/S	378	311	0.24	4.5×10^{14}	0.35	0.46	35	39.4	36.4
Noncompl.	W	288	270	0.023	5.9×10^{14}	0.53	0.55	25	24.9	24.4
	W/S	470	460	0.24	4.5×10^{14}	0.19	0.2	35	45.3	44.7

ADVANCED FUNCTIONAL MATERIALS

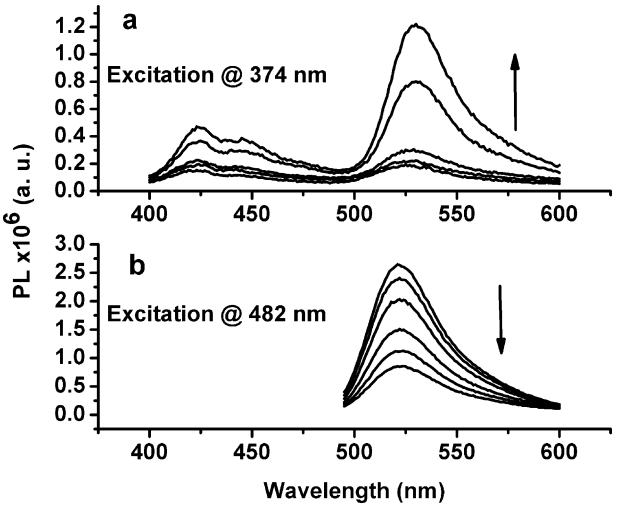

Figure 10. PL emission spectra of complementary DNA:PNA-Flu* (1×10^{-7} M) assay at various CCP concentrations (5×10^{-7} M to 1.6×10^{-6} M), showing the dominant FRET process when the excitation wavelength is 374 nm (a) and the quenching of fluorescein (Flu*–Flu*) and (Flu*–CCP) when the excitation wavelength is 482 nm (b). The arrows show the increase or reduction of the fluorescein emission upon addition of the CCP.

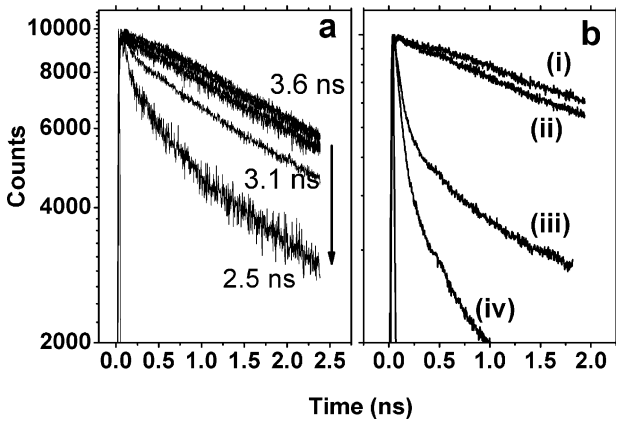

Figure 11. a) Decay profile of the fluorescein in PNA-Flu*as a function of CCP loading ($\lambda_{exc} = 482$ nm). b) Decay profile of the fluorescein in various structures: i) PNA-Flu*, ii) hybridized DNA/PNA-Flu*, iii) hybridized DNA:PNA-Flu*/CCP, and iv) hybridized DNA:PNA-Flu*/CCP/surfactant ($\lambda_{exc} = 374$ nm).

reduces the sensitivity of DNA detection. Unfortunately, the surfactant does not reduce this process. The strong long-range electrostatic force still causes DNA:PNA-Flu* aggregation with the CCP even in the presence of the surfactant, causing fluorescein–fluorescein quenching. Furthermore, the increase in the isolated polymer chain concentration generated by the surfactant may lead to a dynamic quenching of the Flu* with the CCP, which again increases fluorescein quenching. Another possible quenching mechanism is PCT, a process that depends on the relative positions of the orbital energy levels of the donor and acceptor. When the energy levels of the acceptor are not contained within the orbital energies of the donor, donor excitation may lead to PCT.[24,37] In this case excitation of the acceptor would lead to a charge-separated state by means of hole transfer to the donor.[38] However, this process is not the dominant one in our experiment as the surfactant has no influence on it (the surfactant shell would be assumed to block the very short range charge transfer) and this is probably due to the relatively high acceptor concentration used in this experiment, which leads to more pronounced Flu* self-quenching.[24] This is consistent with the literature,[22] where Texas Red (TR), which is not expected to show PCT, gave 18-fold signal amplification when dilute, compared to only 2-fold in the absence of the dilution. The quenching of fluorescein was confirmed by time-resolved experiments, in which the fluorescein emission decay at 520 nm was monitored as a function of CCP concentration using direct excitation of the fluorescein at a wavelength of 482 nm. Figure 11a shows the decay time of the fluorescein in the complementary DNA/PNA-Flu as a function of CCP loading. The lifetime decays were fitted with three exponential terms to obtain mean square error (χ^2) ≈ 1. However, at low CCP loading the quenching is very low and a mono-exponential term is adequate to obtain a good fit. An average lifetime of 3.6 ns was obtained for fluorescein at a CCP loading concentration below 5×10^{-7} M. At higher CCP concentration a second fast decay component was observed, which we ascribed to the fluorescein quenching by aggregation.[24] The slow component drops to 3.1 ns and 2.5 ns at CCP concentrations of 1.6×10^{-6} M and 3×10^{-6} M, respectively. The fluorescein emission decay was also examined in different structures: i) pure PNA-Flu, ii) hybridized (complementary) DNA:PNA-Flu, iii) DNA:PNA-Flu/CCP, and iv) DNA:PNA-Flu/CCP/surfactant (Fig. 11b). The measured decay time for pure PNA-Flu (i) was 3.6 ns; after hybridization with complementary DNA (ii) the decay time decreased to 3.28 ns. Upon addition of CCP (4×10^{-6} M) (iii) the decay shows a strong quenching and the slow component decreases to 2.17 ns. Adding surfactant to the CCP (iv) further increases the Flu* quenching and the slow component decreases to 1.3 ns, owing to the increased effectiveness, that is, increased concentration, of isolated CCP. The quenching processes of the label chromophores are not well understood and a reduction of this quenching is extremely important to further enhance the detection sensitivity of the assay. It should be noted that in order to reduce this effect we should reduce the CCP concentration to its lowest possible limit.

3. Conclusions

Nonionic surfactant enhances the detection of a target DNA sequence. The surfactant enhances both the sensitivity and the selectivity of the detection and provides higher accuracy without adding extra complication to the detection system. A small-molecule nonionic surfactant is best for this purpose. Complete hybridization is also a key factor in efficient DNA detection. Quenching of CCP by ssDNA can be ascribed to

i)=static quenching by forming a complex in the ground state, which reduces the number of isolated polymer chains available for FRET; ii) quenching by charge transfer in the excited state (contact quenching), which competes with the FRET and reduces the energy transfer; and iii) CCP–CCP quenching, which would arise if CCP aggregates were formed by nucleation on the DNA. Surfactant provides a high concentration of isolated polymer chain CCP donors, where the effect of the static quenching by free DNA has less influence on the sensitivity. Surfactant also encapsulates CCP within micelles, reducing the charge-transfer process. While static quenching is very efficient in the CCP/ssDNA system, it becomes less efficient in the CCP/DNA: PNA-Flu system. Two possible explanations of this behavior are that i) the hybridized DNA-PNA is helical, which reduces the perfect contact with the CCP found for ssDNA, and ii) FRET has a longer range than the charge transfer and takes place prior to the charge-transfer process. Surfactant increases CCP quantum yield in water and hence increases the Förster radius for FRET. Surfactant also eliminates quenching by the hybridization buffer (the phosphate in our case) and reduces dramatically the hydrophobic interaction between CCP and PNA-Flu, which enhances the selectivity. Time-resolved analysis clearly differentiates the particular effect brought about by DNA:PNA-Flu assays from other quenching processes that lead to an underestimate of the rate of FRET.

4. Materials and Methods

The CCP used was the cationic water-soluble conjugated polymer poly{[9,9-bis[*N*,*N*,*N*-trimethylammonium)hexylfluorene]-*co*-1,4-phenylene diiodide} **1**, molecular weight around 3000 g mol^{-1},[39] which is about five repeat units. The nonionic *n*-dodecylpentaoxyethylene glycol ether ($C_{12}E_5$) **2** (Scheme 1) was purchased from Aldrich and diluted to the required concentration using distilled and deionized water from a Millipore filtration system (18 MΩ/□). A 12-base fluorescein-labeled PNA probe was obtained from Applied Biosystems, with the base sequence Flu-OO-AGT-AAC-TCA-AGT (Scheme 1, **3**). High purity salt free (HPSF)-purified complementary and noncomplementary DNA sequences to the PNA-Flu* (Fig. 1, **4**,**5**) were obtained from MWG Biotech. The concentrations of the PNA-Flu* and DNAs were determined by measuring the absorbance at 260 nm in 3 mL quartz cells using a PerkinElmer Lambda 19 spectrophotometer. Photoluminescence was measured using a Jobin Yvon Fluorolog spectrophotometer. An equimolar amount (8×10^{-7} M) of PNA-Flu* and either complementary **4** or noncomplementary **5** ssDNAs were mixed, and each mixture was annealed at 70 °C for 20 min before being cooled very slowly to allow the hybridization process to occur. Hybridization was accomplished in 10 mM phosphate buffer (pH 7.4). The hybridized complexes were further diluted to the desired concentrations during the detection.

The detection was carried out by adding CCP to the complementary or noncomplementary assay or to the hybridized ssDNA/PNA-Flu* in small amounts (2×10^{-7} M) and optimizing the energy transfer to PNA-Flu*. In the assay containing surfactant, first a small quantity (1×10^{-8} M) of the mixture of the CCP and the nonionic surfactant was added, followed by CCP without surfactant until maximum FRET ratio was obtained. It is very important to follow this method in order to observe a strong enhancement of both sensitivity and selectivity. The reason for this method is in order to break up polymer aggregations without forming large micelles around the isolated polymer chains. Initially the CCP and surfactant mixture tend to produce isolated polymer chains surrounded by a thick micelle wall, which increases the CCP emission and also enhances the acceptor emission but the FRET ratio remains constant or decreases (because the CCP PL emission overwhelms the fluorescence emission of the acceptor, causing the FRET ratio to decrease). By adding CCP without surfactant in the second stage of optimization, the surfactant in the solution tends to break up the added aggregated CCP instantly and at the same time the newly generated isolated polymer chains interact with the DNA/PNA-Flu* system (before forming a large micelle). This leads to a huge depletion of the donor emission and a large increase in the acceptor emission. In the second, alternative, method, the experiment was carried out in reverse, that is, the acceptor (DNA:PNA-Flu) was added to the diluted donor (CCP or CCP/surfactant). The latter method allows us to study quenching mechanisms using modified Stern–Volmer relationships.

Time-resolved fluorescence decay data were collected using the picosecond time-correlated single photon counting (TCSPC) technique (instrumental resolution function IRF = 23 ps). The excitation source is a picosecond Ti:sapphire laser (MIRA) from Coherent Inc. (vertical polarization, wavelength range 720–1000 nm, 76 MHz repetition rate) coupled to a second harmonic generator (360–500 nm). Emission collected at the polarization magic angle is detected through a double subtractive monochromator by a microchannel plate (MCPT) Hamamatsu model R3809U-50. Signal acquisition was performed using a TCSPC module (Becker & Hickl, model SPC-630). Deconvolution of the fluorescence decays was performed using the Globals WE software package [32].

Received: June 19, 2007
Revised: October 25, 2007
Published online: August 5, 2008

[1] S. B. Primrose, R. M. Twyman, *Principles of Genome Analysis and Genomics*, 3rd ed., Blackwell, Malden, MA **2003**, Ch. 1.
[2] J. Wang, *Nucl. Acids Res.* **2000**, *28*, 3011.
[3] D. Wang, X. Gong, P. S. Heeger, F. Rininsland, G. C. Bazan, A. J. Heeger, *Proc. Natl. Acad. Sci. USA* **2002**, *99*, 49.
[4] T. Ratilainen, A. Holmen, E. Tuite, P. E. Nielsen, B. Norden, *Biochemistry* **2000**, *39*, 7781.

[5] S. R. Mikkelsen, *Electroanalysis* **1996**, *8*, 15.
[6] J. Wang, G. Rivas, X. H. Cai, M. Chicharro, C. Parrado, N. Dontha, A. Begleiter, M. Mowat, E. Palecek, P. E. Nielsen, *Anal. Chim. Acta* **1997**, *344*, 111.
[7] J. Fritz, E. B. Cooper, S. Gaudet, P. K. Sorger, S. R. Manalis, *Proc. Natl. Acad. Sci. USA* **2002**, *99*, 14142.
[8] T. A. Taton, C. A. Mirkin, R. L. Letsinger, *Science* **2000**, *289*, 1757.
[9] H. Li, L. Rothberg, *Proc. Natl. Acad. Sci. USA* **2004**, *101*, 14036.
[10] M. Leclerc, *Adv. Mater.* **1999**, *11*, 1491.
[11] H. A. Ho, M. Boissinot, M. G. Bergeron, G. Corbeil, D. Boudreau, M. Leclerc, *Angew. Chem. Int. Ed.* **2002**, *41*, 1548.
[12] H. A. Ho, K. Doré, M. Boissinot, M. G. Bergeron, R. M. Tanguay, D. Boudreau, M. Leclerc, *J. Am. Chem. Soc.* **2005**, *127*, 12673.
[13] S. A. Kushon, K. Ley, K. Bradford, R. M. Jones, D. McBranch, D. Whitten, *Langmuir* **2002**, *18*, 7245.
[14] B. S. Gaylord, A. J. Heeger, G. C. Bazan, *Proc. Natl. Acad. Sci. USA* **2002**, *99*, 10954.
[15] P. E. Nielson, M. Engholm, R. H. Berg, O. Burchardt, *Science* **1991**, *254*, 1497.
[16] M. Engholm, O. Burchardt, P. E. Nielson, R. H. Berg, *J. Am. Chem. Soc.* **1992**, *114*, 1895.
[17] H. A. Al Attar, A. P. Monkman, *J. Phys. Chem. B* **2007**, *111*, 12418.
[18] S. A. Kushon, K. Bradford, V. Marin, C. Suhrada, B. A. Armitage, D. McBranch, D. Whitten, *Langmuir* **2003**, *19*, 6456.
[19] Q.-H. Xu, B. S. Gaylord, S. Wang, G. C. Bazan, D. Moses, A. J. Heeger, *Proc. Natl. Acad. Sci. USA* **2004**, *101*, 11634.
[20] J. W. Eastman, S. J. Rehfeld, *J. Phys. Chem.* **1970**, *74*, 1438.
[21] F. P. Schwarz, S. D. Wasik, *Anal. Chem.* **1976**, *48*, 524.
[22] B. Liu, G. C. Bazan, *J. Am. Chem. Soc.* **2004**, *126*, **1942**.
[23] S. Wang, B. S. Gaylord, G. C. Bazan, *J. Am. Chem. Soc.* **2004**, *126*, 5446.
[24] B. Liu, G. C. Bazan, *J. Am. Chem. Soc.* **2006**, *128*, 1188.
[25] J. J. Lavigne, D. L. Broughton, J. N. Wilson, B. Erdogan, U. H. F. Bunz, *Macromolecules* **2003**, *36*, 7409.
[26] H. D. Burrows, V. M. M. Lobo, J. Pina, M. L. Ramos, M. J. de Seixas, A. J. M. Valente, M. J. Tapia, S. Pradhan, U. Scherf, *Macromolecules* **2004**, *37*, 7425.
[27] M. Yan, L. J. Rothberg, E. W. Kwock, T. M. Miller, *Phys. Rev. Lett.* **1995**, *75*, **1992**.
[28] U. Menge, P. Lang, G. Findenegg, H. P. Strunz, *J. Phys. Chem. B* **2003**, *107*, 1316.
[29] M. Knaapila, L. Almásy, V. M. Garamus, C. Pearson, S. Pradhan, M. C. Petty, U. Scherf, H. D. Burrows, A. P. Monkman, *J. Phys. Chem. B* **2006**, *110*, 10248.
[30] T. Strachan, A. P. Read, *Human Molecular Genetics*, 3rd ed., Garland Science Publishing, New York **2003**, Ch. 1.
[31] H. A. Al Attar, J. Norden, S. O'Brien, A. P. Monkman, *Biosens. Bioelectron.* **2008**, *23*, 1466.
[32] E. Gratton, J. Beechem, *Globals WE* (software), Laboratory for Fluorescence Dynamics, University of California, Irvine, CA **2004**.
[33] J. R. Lakowicz, *Principles of Fluorescence Spectroscopy*, Plenum, New York **1999**, Ch. 13.
[34] A. E. S. Marras, R. F. Kramer, S. Tyagi, *Nucl. Acids Res.* **2002**, *30*, e122.
[35] L. Chen, D. W. McBranch, H. L. Wang, R. Helgeson, F. Wudl, D. G. Whitten, *Proc. Natl. Acad. Sci. USA* **1999**, *96*, 12287.
[36] J. Wang, D. Wang, E. K. Miller, D. Moses, G. C. Bazan, A. J. Heeger, *Macromolecules* **2000**, *33*, 5153.
[37] a) N. S. Sariciftci, L. Smilowitz, A. J. Heeger, F. Wudl, *Science* **1992**, *258*, 1474. b) K. R. J. Thomas, A. L. Thompson, A. V. Sivakumar, A. C. Bardeani, S. Thayumanavan, J. Am, Chem, Soc, **2005**, *127*, 373.
[38] J. Cornil, V. Lemaue, M. C. Steel, H. Dupin, A. Burquel, D. Beljonne, J. L. Brédas, in *Organic Photovoltaics* (Eds: S. J. Sun, N. S. Sariciftci), Taylor and Francis, Boca Raton, FL **2005**, p. 161.
[39] U. Scherf, W. List, *Adv. Mater.* **2002**, *14*, 477.